Strong cosmic censorship for the massless charged scalar field in the Reissner-Nordstrom–de Sitter spacetime

Yuyu Mo,[1,2,*] Yu Tian,[3,†] Bin Wang,[1,4,‡] Hongbao Zhang,[2,5,§] and Zhen Zhong[2,‖]

[1]*Center for Gravitation and Cosmology, College of Physical Science and Technology, Yangzhou University, Yangzhou 225009, China*
[2]*Department of Physics, Beijing Normal University, Beijing 100875, China*
[3]*School of Physics, University of Chinese Academy of Sciences, Beijing 100049, China*
[4]*Department of Physics and Astronomy, Shanghai Jiao Tong University, Shanghai 200240, China*
[5]*Theoretische Natuurkunde, Vrije Universiteit Brussel, and The International Solvay Institutes, Pleinlaan 2, B-1050 Brussels, Belgium*

(Received 16 August 2018; published 19 December 2018)

It has recently been shown that the strong cosmic censorship conjecture can be violated by the massless neutral scalar field in the nearly extremal Reissner-Nordstrom–de Sitter black hole. However, the formation of such a black hole by gravitational collapse necessitates the presence of the charged sector on top of the Einstein-Maxwell system. Thus, we numerically calculate the quasinormal modes for a massless charged scalar field in the Reissner-Nordstrom–de Sitter spacetime by generalizing the characteristic formulation to the charged case. As a result, the strong cosmic censorship is recovered by our massless charged scalar field except in the highly extremal limit $Q \to Q_m$, where the violation still occurs when the scalar field is appropriately charged.

DOI: 10.1103/PhysRevD.98.124025

I. INTRODUCTION AND MOTIVATION

As is well known, a variety of versions of singularity theorems tell us that spacetime singularity can be formed generically by the gravitational collapse of suitable matter distribution [1,2]. Such a formation of singularity indicates that general relativity breaks down near the singularity and will be replaced by the so-called complete quantum theory of gravity. In particular, if the formed singularity is timelike, general relativity will lose its predictive power because of the region of spacetime under consideration, whose past domain of influence will hit the singularity. With this in mind, Penrose proposed his strong cosmic censorship hypothesis (SCC) to maintain the predictability of classical general relativity. The SCC, in essence, states that the gravitational collapse of generic initial distribution for suitable matter only leads to a spacelike or lightlike singularity.

The timelike singularity in the eternal Kerr and Reissner-Nordstrom black holes appears to violate the SCC. However, this is not the case because the remnant fields are generically present, along with the real-life black hole formed from the gravitational collapse. These remnant fields, which are demonstrated to have an inverse power-law decay behavior outside of the black hole, will be amplified when propagated along the Cauchy horizon due to the exponential blueshift effect. As a result, the Cauchy horizon becomes singular such that one cannot extend across the would-be Cauchy horizon to the spacetime region with the timelike singularity.

But the above argument does not apply to the black holes in de Sitter spacetime because the remnant fields instead have an exponential decay behavior outside of the black hole [3–9]. Accordingly, the extendibility of the Cauchy horizon depends delicately on the competition between the exponential decay behavior outside of the black hole and the exponential blueshift amplification along the Cauchy horizon. As shown in [10], the blueshift effect wins for the remnant fields around the Kerr–de Sitter black hole, so the SCC is respected. On the other hand, when one considers the remnant massless neutral scalar field around the Reissner-Nordstrom–de Sitter (RNdS) black hole, the exponential decay effect wins in some regime of the parameter space under consideration such that the SCC is violated [11]. Such a violation becomes more severe for the coupled electromagnetic and gravitational perturbations [12]. However, taking into account the unavoidable presence of charged remnant fields in the dynamical formation of the RNdS black hole, Hod found that the SCC is restored at least by the scalar field with a sufficiently large charge and mass [13]. The purpose of this paper is to see what happens to the SCC if one charges the massless scalar field considered in [11]. In this case, Hod's analytic analysis does not work, so we are

*yymo@mail.bnu.edu.cn
†ytian@ucas.ac.cn
‡wangb@yzu.edu.cn
§hzhang@vub.ac.be
‖zhenzhong@mail.bnu.edu.cn

required to numerically calculate the low-lying quasinormal modes (QNMs) for the massless charged scalar field in the RNdS black hole background. Our result shows that the SCC is recovered by our massless charged scalar field except in the highly extremal limit, where the violation can still occur when the charge of our scalar field is tuned to some appropriate regime.

This paper is organized as follows. In the subsequent section, we develop the relationship between the QNMs and the SCC for the charged scalar field in RNdS background. In Sec. III, after introducing our numerical scheme for the time evolution of the charged scalar field by the double null coordinates, we present the relevant numerical results about the low-lying QNMs for the massless charged scalar field and the implications to the SCC. We conclude our paper in the last section with some discussions.

II. QUASINORMAL MODES AND STRONG COSMIC CENSORSHIP

Let us start with the four-dimensional RNdS black hole

$$ds^2 = -f(r)dt^2 + \frac{dr^2}{f(r)} + r^2(d\theta^2 + \sin^2\theta d\phi^2),$$
$$A_a = -\frac{Q}{r}(dt)_a, \tag{1}$$

where the blackening factor

$$f(r) = 1 - \frac{2M}{r} + \frac{Q^2}{r^2} - \frac{\Lambda r^2}{3} \tag{2}$$

with M and Q the mass and charge of the black hole, and Λ the positive cosmological constant. If the cosmological, event, and Cauchy horizons are designated as r_c, r_+, and r_- individually, then the blackening factor can also be written as

$$f(r) = \frac{\Lambda}{3r^2}(r_c - r)(r - r_+)(r - r_-)(r - r_o) \tag{3}$$

with $r_o = -(r_c + r_+ + r_-)$. In addition, the surface gravity at each horizon r_h is given by $\kappa_h = |\frac{1}{2}f'(r_h)|$. Whence, we have

$$\kappa_c = \frac{\Lambda}{6r_c^2}(r_c - r_+)(r_c - r_-)(r_c - r_o),$$
$$\kappa_+ = \frac{\Lambda}{6r_+^2}(r_c - r_+)(r_+ - r_-)(r_+ - r_o),$$
$$\kappa_- = \frac{\Lambda}{6r_-^2}(r_c - r_-)(r_+ - r_-)(r_- - r_o),$$
$$\kappa_o = \frac{\Lambda}{6r_o^2}(r_c - r_o)(r_+ - r_o)(r_- - r_o). \tag{4}$$

Now suppose that the behavior of the charged scalar field in such a curved spacetime is governed by the following Klein-Gordon equation:

$$[(\nabla_a - iqA_a)(\nabla^a - iqA^a) - m^2]\Psi = 0, \tag{5}$$

which can be written explicitly as

$$-\frac{\partial_t^2\Psi}{f} + \frac{1}{r^2}\partial_r(r^2 f\partial_r\Psi) + \frac{1}{r^2}\left[\frac{1}{\sin\theta}\partial_\theta(\sin\theta\partial_\theta\Psi) + \frac{1}{\sin^2\theta}\partial_\phi^2\Psi\right] - \frac{2iqQ}{rf}\partial_t\Psi + \frac{(qQ)^2}{r^2 f}\Psi - m^2\Psi = 0 \tag{6}$$

with m and q the mass and charge of the scalar field. Associated with an arbitrary solution to this equation of motion, not only is there a gauge transformation $(A_a, \Psi) \to (A_a + \nabla_a\lambda, e^{iq\lambda}\Psi)$, but also a conserved current given by

$$j^a = i[\bar{\Psi}(\nabla^a - iqA^a)\Psi - \Psi(\nabla^a + iqA^a)\bar{\Psi}]. \tag{7}$$

Due to the symmetry of the background and the linearity of the dynamics, it is sufficient for us to consider the scalar field as

$$\Psi = \frac{\psi(r)}{r}Y_{lm}(\theta,\phi)e^{-i\omega t}. \tag{8}$$

Plugging it into the above equation of motion, we wind up with the effective equation

$$\frac{d^2\psi}{dr_*^2} + \{[\omega - \Phi(r)]^2 - V(r)\}\psi = 0 \tag{9}$$

for the radial function, where the tortoise coordinate r_* is defined as $dr_* = \frac{dr}{f}$ with the electric potential $\Phi(r) = \frac{qQ}{r}$ and the effective potential $V(r) = \frac{f[rf' + l(l+1) + m^2r^2]}{r^2}$. It obviously follows that the radial function behaves as

$$\psi \sim e^{\pm i[\omega - \Phi(r_h)]r_*} \tag{10}$$

near any one of the horizons r_h. Now let us consider the regime between the event and cosmological horizons, where r_* can be integrated out as

$$r_* = -\frac{1}{2\kappa_c}\ln\left(1 - \frac{r}{r_c}\right) + \frac{1}{2\kappa_+}\ln\left(\frac{r}{r_+} - 1\right) - \frac{1}{2\kappa_-}\ln\left(\frac{r}{r_-} - 1\right) + \frac{1}{2\kappa_o}\ln\left(1 - \frac{r}{r_o}\right). \tag{11}$$

If we impose the following boundary conditions,

$$\psi \sim e^{-i[\omega - \Phi(r_+)]r_*} \quad r \to r_+, \qquad \psi \sim e^{i[\omega - \Phi(r_c)]r_*} \quad r \to r_c, \tag{12}$$

namely, the ingoing boundary condition near the event horizon and the outgoing boundary condition near the

cosmological horizon, then the equation of motion will give rise to a set of discrete frequencies, which are the so-called QNMs. It is noteworthy that the spectrum of QNMs for the scalar field with the charge q is related to that with the charge $-q$ by the minus complex conjugation. So when the scalar is neutral, the spectrum of QNMs is symmetric with respect to the imaginary axis on the ω plane. As we see in the next section, this symmetry will be broken in the presence of the charge.

On the other hand, with the above ingoing boundary condition near the event horizon, the solution inside of the black hole generically has both the outgoing and ingoing modes near the Cauchy horizon. By performing the gauge transformation with $d\lambda = \frac{Q}{r} dr_*$, and the coordinate transformation to the outgoing coordinates with u defined as $u = t - r_*$, which allows us to analytically continue our metric and electric potential across the Cauchy horizon, the outgoing and ingoing modes can be expressed as

$$\psi_o \sim e^{-i\omega u}, \qquad \psi_i \sim e^{-i\omega u}(r - r_-)^{\frac{i[\omega - \Phi(r_-)]}{\kappa_-}}, \qquad r \to r_- \tag{13}$$

near the Cauchy horizon, respectively. Obviously, the potential nonsmoothness near the Cauchy horizon comes from the ingoing mode ψ_i. As detailed in [10], one can extend this mode across the Cauchy horizon such that the SCC is violated if and only if it has a locally square integrable derivative, belonging to the Sobolev space H^1_{loc}, which requires

$$\beta \equiv -\frac{\text{Im}(\omega)}{\kappa_-} > \frac{1}{2}. \tag{14}$$

Put another way, if one can find a quasinormal mode with $\beta < \frac{1}{2}$, then the SCC is preserved. So for this purpose, we are only required to focus on the lowest-lying quasinormal mode.

III. NUMERICAL SCHEME AND RELEVANT RESULTS

A. Numerical scheme

Regarding the QNMs of the charged scalar field in the RNdS black hole, early works include [14,15]. Those works focused on the superradiance instability, and the numerical scheme they used is the general initial value integration. Below we also extract the QNMs by the time domain analysis, but instead we evolve our initial data by the characteristic formulation, which was proposed originally in [16]. This characteristic formulation has been adopted in various case studies [17–21]. We generalize this formulation to our charged scalar field. To proceed, as demonstrated in Fig. 1, we first make the coordinate transformation to the double null coordinates (u, v), with u defined before and v defined as $v = t + r_*$. Accordingly, the metric reads

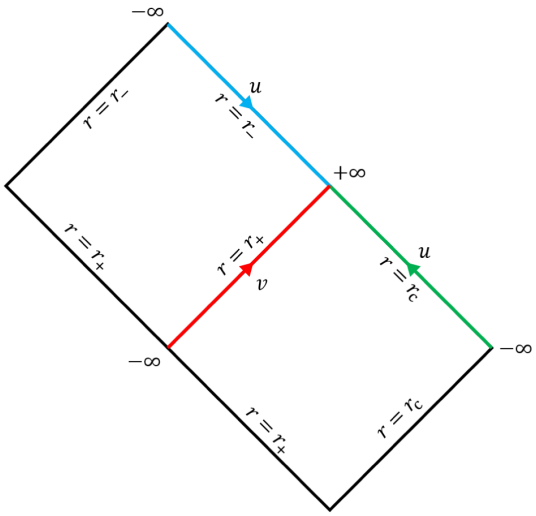

FIG. 1. Penrose diagram for the RNdS black hole with u and v defined as $u = t - r_*$ and $v = t + r_*$. The red line, blue line, and green line denote the black hole event horizon, Cauchy horizon, and cosmological horizon individually.

$$ds^2 = -f du dv + r^2(d\theta^2 + \sin^2\theta d\phi^2). \tag{15}$$

In addition, we would also like to make the gauge transformation $d\lambda = \frac{Q(2r - r_c - r_+)}{r(r_c - r_+)} dr_*$ such that the electric potential reads

$$A_a = -\frac{Q(r - r_+)}{r(r_c - r_+)}(du)_a + \frac{Q(r - r_c)}{r(r_c - r_+)}(dv)_a. \tag{16}$$

If we expand the scalar field as

$$\Psi = \frac{\psi(u, v)}{r} Y_{lm}(\theta, \phi), \tag{17}$$

then the resultant Klein-Gordon equation can be expressed as

$$0 = -4\partial_u\partial_v\psi - 4i\Phi(r)\left(\frac{r_c - r}{r_c - r_+}\partial_u\psi + \frac{r - r_+}{r_c - r_+}\partial_v\psi\right) - U(r)\psi, \tag{18}$$

where $U(r) = \frac{4\Phi^2(r)(r - r_c)(r - r_+)}{(r_c - r_+)^2} + \frac{f}{r^2}[(l(l+1) + f'r + m^2r^2 + i\frac{\Phi(r)r(r_c + r_+)}{r_c - r_+}]$. Whence, it is not hard to see that the QNMs behave as $e^{-i\omega v}$ near r_+ and $e^{-i\omega u}$ near r_c. This is actually the reason why we have made the above gauge transformation.

To numerically solve the above partial differential equation, we approximate it at the point $O(u_0 + \frac{\Delta}{2}, v_0 + \frac{\Delta}{2})$ to the order of $O(\Delta^2)$ in the following way:

$$\partial_u\partial_v\psi|_O \to \frac{\psi(N) - \psi(E) - \psi(W) + \psi(S)}{\Delta^2}, \tag{19}$$

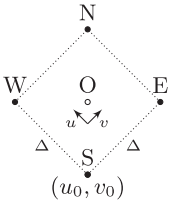

FIG. 2. Finite difference scheme to obtain the data at N from the data at E, W, and S.

$$\partial_u \psi|_O \to \frac{\psi(N)+\psi(W)-\psi(E)-\psi(S)}{2\Delta}, \tag{20}$$

$$\partial_v \psi|_O \to \frac{\psi(N)+\psi(E)-\psi(W)-\psi(S)}{2\Delta}, \tag{21}$$

$$\psi(O) \to \frac{\psi(E)+\psi(W)}{2}, \tag{22}$$

where, as depicted in Fig. 2, N, E, W, and S correspond individually to the points $(u_0+\Delta, v_0+\Delta)$, $(u_0, v_0+\Delta)$, $(u_0+\Delta, v_0)$, and (u_0, v_0). With this approximation, the equation of motion gives rise to

$$\psi(N) = \left(1+i\frac{\Phi(r)\Delta}{2}\right)^{-1}\left[-\left(1-i\frac{\Phi(r)\Delta}{2}\right)\psi(S)\right. \tag{23}$$

$$-i\frac{(2r-r_c-r_+)\Phi(r)\Delta}{2(r_c-r_+)}(\psi(E)-\psi(W))$$
$$\left.+\left(1-\frac{U(r)\Delta^2}{8}\right)(\psi(E)+\psi(W))\right], \tag{24}$$

where r is evaluated at the point O; thus, it can be solved by $r_*(r) = \frac{1}{2}(v_0-u_0)$. As illustrated in Fig. 3, to reduce the computing time, we adopt a parallel evolution along the time t slice within the diamond under consideration. In addition, in our numerical evolution, the initial value for our scalar field is set as follows:

$$\psi(0,v) = 0,$$
$$\psi(u,0) = \frac{1}{\sqrt{2\pi}\sigma}e^{-\frac{(u-u_c)^2}{2\sigma^2}}, \tag{25}$$

with σ and u_c as the width and center of the Gaussian wave packet. Then, we extract the spectrum of low-lying QNMs from the N equally elapsed late-time data $\hat{\psi}(t_p) = \psi(t_0+p\Delta, r_*=0)$ using the Prony method [22]. The convergence of our numerics is examined by decreasing the evolution step length Δ. We have also tested our numerics by reproducing the relevant results reported in the previous literature, such as [11,14,15]. Below we focus only on the massless scalar field, although the prescribed

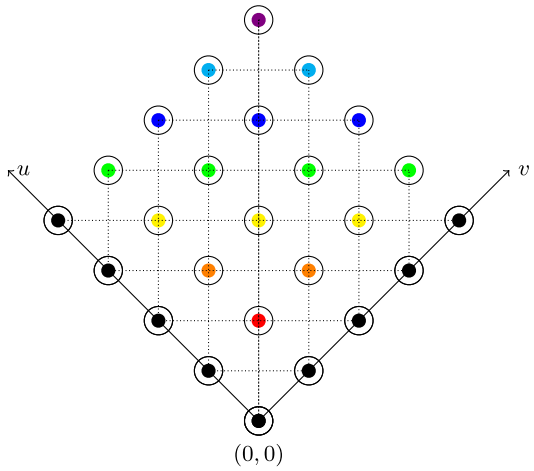

FIG. 3. Diamond parallel evolution scheme, where horizontal and vertical lines correspond to the time t slice and equal r line, respectively.

numerical scheme can be applied equally to the massive case. In addition, we work with the units in which $M = 1$.

As a demonstration, we would like to conclude this subsection by depicting the temporal evolution of $\hat{\psi}(t)$ of $q = 0.1$ in Fig. 4 and list the corresponding spectrum of low-lying QNMs in Table I for $\Lambda = 0.02$ and $Q/Q_m = 0.9910$, where Q_m corresponds to the charge of the black hole with $r_+ = r_-$ and n denotes the overtone number, with $n = 1$ representing the fundamental mode. Among others, we see there is a slowly growing unstable mode for $l = 0$ with its real part $\frac{\mathrm{Re}(\omega)}{\kappa_-} \in (\frac{\Phi(r_c)}{\kappa_-} = 0.051966, \frac{\Phi(r_+)}{\kappa_-} = 0.503183)$. Actually, as shown before in [14,15], this kind of unstable mode appears only for $l = 0$ and is always superradiant.

B. Relevant results

Due to the limited computational resources, we have no intention of charting the corresponding spectrum of

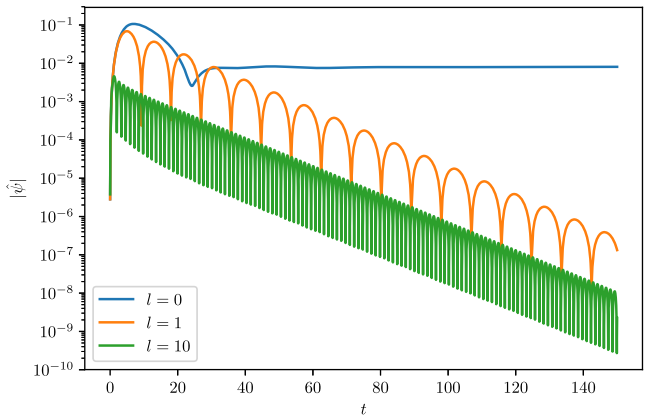

FIG. 4. The temporal evolution of $|\hat{\psi}(t)|$ of $q = 0.1$ for $\Lambda = 0.02$ and $Q/Q_m = 0.9910$.

TABLE I. The low-lying QNMs $\frac{\omega}{\kappa_-}$ of $q = 0.1$ for $\Lambda = 0.02$ and $Q/Q_m = 0.9910$.

n	$l = 0$	$l = 1$	$l = 10$
1	$0.057773 + 0.002227i$	$0.032203 - 0.475118i$	$-14.080 - 0.491i$
2	$1.008291 - 0.520028i$	$2.348530 - 0.499977i$	$14.653 - 0.492i$
3	$-0.452819 - 0.559594i$	$-1.769203 - 0.500762i$	$-14.059 - 1.474i$
4	$0.598660 - 0.834292i$	$-0.033667 - 1.435223i$	$14.633 - 1.476i$

low-lying QNMs for the whole parameter space. Actually, as demonstrated in [11], only in the near extremal RNdS black hole is the SCC violated by the massless neutral scalar field, where the dominant criminal modes can be the de Sitter mode, the photon sphere mode, or the near extremal mode, depending on the specific parameter value in the moduli space. With this in mind, we simply investigate some representative points in the moduli space, which also suffices for our purpose. In particular, the following representative points are chosen to facilitate the comparison, if necessary, with the result presented in [11].

We first present the lowest-lying QNMs in Fig. 5 for the case of $\Lambda = 0.02$ and $Q/Q_m = 0.9950$, where the SCC would be violated by the $l = 1$ dominant de Sitter mode if the massless scalar field was uncharged. However, once we charge the scalar field, the $l = 0$ trivial zero mode becomes nontrivial. In particular, it demonstrates the superradiant instability in the small charge regime and then stabilizes when the charge is large enough, which is consistent with the previous observation made in [14,15]. But no matter if it is unstable or stable, this $l = 0$ zero mode still lies well above the $-1/2$ horizontal threshold line, thus saves the SCC.

Now let us turn to the case of $\Lambda = 0.14$ and $Q/Q_m = 0.9950$, where the SCC would be violated by the photon sphere dominant mode if the massless scalar field was uncharged. As shown in Fig. 6, the $l = 0$ trivial zero mode still becomes nontrivial once the scalar field is charged, although it does not demonstrate the superradiance instability anymore, consistent with the observation made in [14,15] that a large cosmological constant stabilizes the system. Similarly, in the presence of the charge, this mode keeps the SCC from being violated again. As an aside, there is an obvious nonsmoothness for the behavior of the $l = 0$ dominant mode as one cranks up the charge. As demonstrated in Fig. 7, such a nonsmoothness arises from the fact that the $l = 0$ near extremal mode takes over the dominant position from the $l = 0$ zero mode when the charge is large enough.

Next let us see what happens to the case of $\Lambda = 0.14$ and $Q/Q_m = 0.9985$, where the SCC would be violated

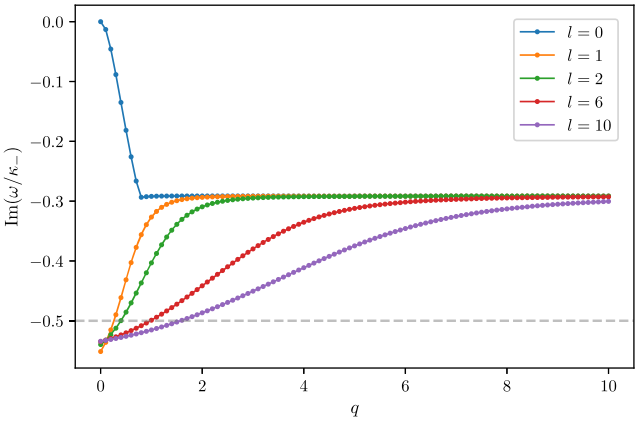

FIG. 6. The lowest-lying QNMs for $\Lambda = 0.14$ and $Q/Q_m = 0.9950$.

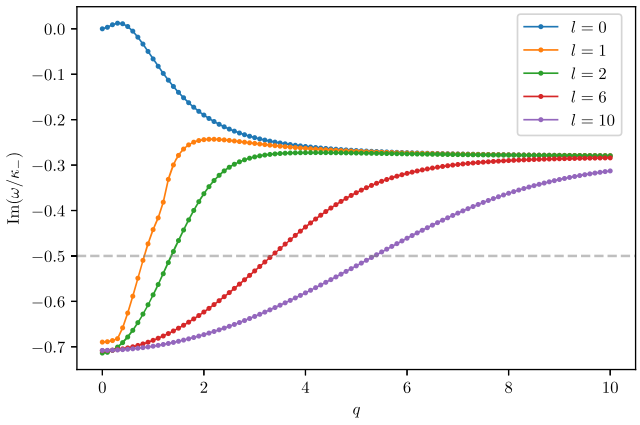

FIG. 5. The lowest-lying QNMs for $\Lambda = 0.02$ and $Q/Q_m = 0.9950$.

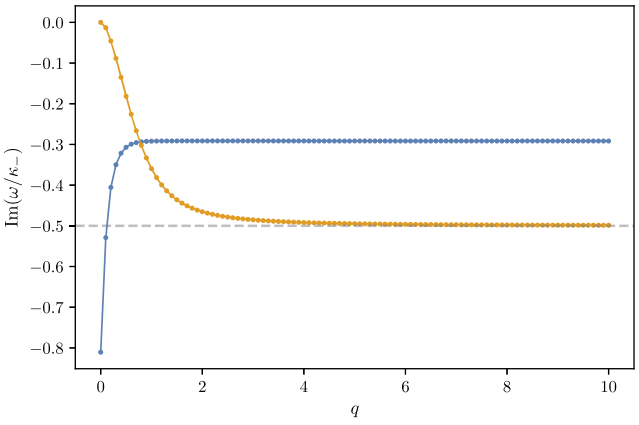

FIG. 7. The $l = 0$ dominant and subdominant QNMs for $\Lambda = 0.14$ and $Q/Q_m = 0.9950$, where the orange points and blue points denote the zero mode and near extremal mode, respectively.

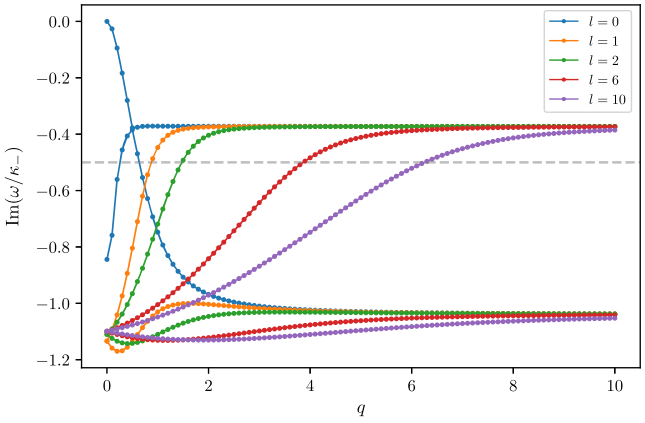

FIG. 8. The dominant and subdominant QNMs for $\Lambda = 0.14$ and $Q/Q_m = 0.9985$.

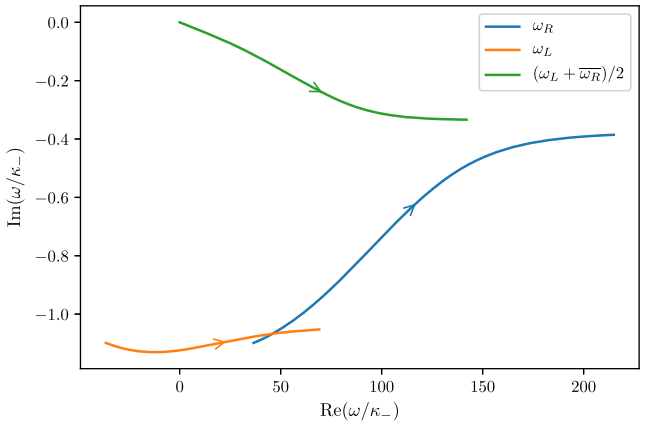

FIG. 9. The symmetry breaking of the $l = 10$ left and right photon sphere modes for $\Lambda = 0.14$ and $Q/Q_m = 0.9985$. The orange points denote the left photon sphere modes ω_L, the blue points denote the right photon sphere modes ω_R, and the green points denote $(\omega_L + \bar{\omega}_R)/2$, where the arrow indicates the increase of the charge q from 0 to 10.

by the $l = 0$ dominant extremal mode if the massless scalar field was uncharged. As such, we would like to depict the corresponding dominant and subdominant QNMs in Fig. 8. As one can see, due to the $l = 0$ nontrivial zero mode in the presence of the charge, there is no violation of the SCC. In addition, it is noteworthy that the presence of the charge breaks the left and right symmetry between the $l \neq 0$ photon sphere modes with respect to the imaginary axis on the ω plane. To be more precise, as illustrated in Fig. 9 for the $l = 10$ photon sphere modes, the magnitude of both the real and imaginary parts of $\omega_L + \overline{\omega_R}$ increases from zero as the charge q varies from 0 to 10.

Comparing Figs. 6 and 8, one can see that the minimum of $\frac{\mathrm{Im}(\omega)}{\kappa_-}$ for the dominant QNMs decreases when the charge of the black hole is increased toward the extremal limit. Actually, this is the case. Moreover, the SCC is still violated in such a limiting case [23]. To see this explicitly,

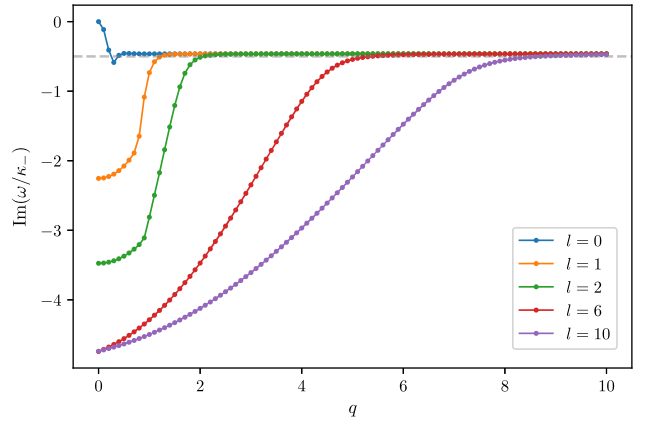

FIG. 10. The lowest-lying QNMs for $\Lambda = 0.14$ and $Q/Q_m = 0.9999$.

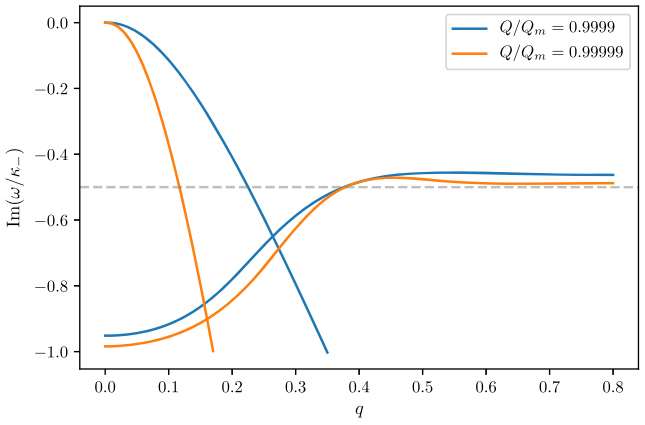

FIG. 11. The violation regime for $\Lambda = 0.14$ gets bigger when the extremal limit is approached.

we depict the lowest-lying QNMs in Fig. 10 for $\Lambda M^2 = 0.14$ and $Q/Q_m = 0.9999$. Obviously, although the SCC is respected in the regime where the charge of the scalar field is sufficiently small or sufficiently large, the violation of the SCC still occurs when the scalar field is appropriately charged within the narrow regime. Furthermore, we zoom in on this violation regime in Fig. 11, which demonstrates that this violation regime becomes bigger when one approaches the extremal limit. In particular, the minimal violation charge gets smaller while the maximal violation charge remains almost unchanged. This indicates that the maximal violation charge may converge to a finite value in the extremal limit. Namely, once the charge of the scalar field is larger than this value, the SCC is always respected [25].

IV. CONCLUSION AND DISCUSSION

To address the SCC in the presence of the massless charged scalar field on top of the RNdS black hole, we have succeeded in calculating the corresponding low-lying

QNMs using the time domain analysis. To this end, we generalize the characteristic formulation to the charged case in the double null coordinates. As a result, we find that the presence of the massless charged scalar field can recover the SCC in the RNdS black hole except in the highly extremal limit, where the violation can still occur when the scalar field is appropriately charged.

In addition, among others, our numerical result also demonstrates two interesting patterns. First, the $l = 0$ dominant mode seems to always dominate over the $l \neq 0$ dominant modes. Second, it seems that the imaginary parts of different l modes converge to some discrete values in the large q limit. Both of these issues beg an analytic analysis. So far, our investigation has been restricted at the linear level. So not only is it intriguing to see how the would-be Cauchy horizon becomes singular, but it is also important to figure out the superradiant instability induced final state using the fully nonlinear numerical simulation. We hope to address some of these topics in the near future.

ACKNOWLEDGMENTS

This work is partially supported by NSFC through Grants No. 11475179, No. 11675015, and No. 11775022, as well as by FWO-Vlaanderen through Projects No. G020714N, No. G044016N, and No. G006918N. Y. T. is also supported by the "Strategic Priority Research Program of the Chinese Academy of Sciences" through Grant No. XDB23030000. B. W. acknowledges support from NSFC through Grant No. 11575109. H. Z. is supported by the Vrije Universiteit Brussel through the Strategic Research Program "High-Energy Physics." We would like to thank Vitor Cardoso, Kyriakos Destounis, and Aron Jansen for numerous communications on various issues related to this project. Thanks are also due to Pau Figueras and Ran Li for their valuable discussions on our numerical scheme. We are also grateful to Shahar Hod, Jorge Santos, and Xiaoning Wu for their helpful discussions on the SCC.

[1] R. Penrose, Gen. Relativ. Gravit. **34**, 1141 (2002).
[2] S. W. Hawking and R. Penrose, Proc. R. Soc. A **314**, 529 (1970).
[3] C. Chambers, Ann. Isr. Phys. Soc. **13**, 33 (1997).
[4] P. R. Brady, C. M. Chambers, W. Krivan, and P. Laguna, Phys. Rev. D **55**, 7538 (1997).
[5] M. Dafermos, Commun. Math. Phys. **332**, 729 (2014).
[6] J. L. Costa, P. M. Girao, J. Natario, and J. D. Silva, Ann. PDE **3**, 8 (2017).
[7] P. Hintz and A. Vasy, J. Math. Phys. (N.Y.) **58**, 081509 (2017).
[8] J. L. Costa and A. T. Franzen, Ann. Inst. Henri Poincaré **18**, 3371 (2017).
[9] P. Hintz, arXiv:1612.04489.
[10] O. J. C. Dias, F. C. Eperson, H. S. Reall, and J. E. Santos, Phys. Rev. D **97**, 104060 (2018).
[11] V. Cardoso, J. L. Costa, K. Destounis, P. Hintz, and A. Jansen, Phys. Rev. Lett. **120**, 031103 (2018).
[12] O. J. C. Dias, H. S. Reall, and J. E. Santos, J. High Energy Phys. 10 (2018) 001.
[13] S. Hod, arXiv:1801.07261.
[14] Z. Zhu, S. Zhang, C. E. Pellicer, B. Wang, and E. Abdalla, Phys. Rev. D **90**, 044042 (2014).
[15] R. A. Konoplya and A. Zhidenko, Phys. Rev. D **90**, 064048 (2014).
[16] C. Gundlach, R. Price, and J. Pullin, Phys. Rev. D **49**, 883 (1994).
[17] P. R. Brady, C. M. Chambers, W. G. Laarakkers, and E. Poisson, Phys. Rev. D **60**, 064003 (1999).
[18] B. Wang, C. Molina, and E. Abdalla, Phys. Rev. D **63**, 084001 (2001).
[19] C. Molina, D. Giugno, E. Abdalla, and A. Saa, Phys. Rev. D **69**, 104013 (2004).
[20] B. Wang, C. Lin, and C. Molina, Phys. Rev. D **70**, 064025 (2004).
[21] J. Lucietti, K. Murata, H. S. Reall, and N. Tanahashi, J. High Energy Phys. 03 (2013) 035.
[22] E. Berti, V. Cardoso, J. A. Gonzalez, and U. Sperhake, Phys. Rev. D **75**, 124017 (2007).
[23] Recently, we were informed by Aron Jansen that they find there is still a violation of SCC when one goes to the $Q \to Q_m$ limit in [24], and he suggested adding such a limiting point in the moduli space for a complete picture. We are grateful to Aron Jansen and his companions for such an improvement.
[24] V. Cardoso, J. L. Costa, K. Destounis, P. Hintz, and A. Jansen, Phys. Rev. D **98**, 104007 (2018).
[25] It is noteworthy that the wiggles found in [26] for some region of the moduli space may change such a picture.
[26] O. J. C. Dias, H. S. Reall, and J. E. Santos, arXiv:1808.04832.